Proceedings of PVP01
2004 5th International Symposium on Computational Technologies
for Fluid/Thermal/Chemical Systems with Industrial Applications
San Diego/La Jolla, California, USA, July 25-29, 2004

34

TREATMENT OF FAST CHEMISTRY IN FDF/LES: IN SITU ADAPTIVE TABULATION

E. van Vliet* **R.O. Fox**
Chemical Engineering Department
Iowa State University
2114 Sweeney Hall
Ames, Iowa, 50011-2230

J.J. Derksen
Kramers Laboratorium voor
Fysische Technologie
Delft University of Technology
Prins Berhardlaan 6
2628 BW Delft, The Netherlands

S.B. Pope
Sibley School of Mechanical
and Aerospace Engineering
Cornell University
240 Upson Hall
Ithaca, New York 14853-7501

ABSTRACT

The feasibility to implement fast-chemistry reactions in a three-dimensional large eddy simulation (LES) of a turbulent reacting flow using a filtered density function (FDF) technique is studied. Low-density polyethylene (LDPE) is used as an representative reaction due to the stiff nature of the ordinary differential equation (ODE's) describing the kinetics. In FDF/LES, the chemistry needs to be evaluated many times for a large number of fictitious particles that are tracked in the flow, and therefore a constraint is put to the CPU time needed to solve the kinetics. Pope (1997) developed an *in situ* adaptive tabulation (ISAT) to treat complex chemistry computationally very efficiently when many evaluations of the chemistry are needed. Kolhapure and Fox (1999) successfully applied ISAT to LDPE using a quasi steady state assumption (QSSA). In the present paper, the aim is to optimize the latest version (ISAT Version 4.0, Pope, 2003) for the full LDPE reaction (i.e. without QSSA), in terms of accuracy and speed up by varying the error tolerance and the number of trees used by ISAT. For this purpose, a pairwise mixing stirred reactor (PMSR) is employed, since it forms a stringent test for the chemistry solver due to the large accessed region of composition space that can be established. For a number of trees of $N_{\text{tree}} = 8$ and an error tolerance of $\varepsilon_{\text{tol}} = 10^{-5}$ the best overall performance of ISAT was obtained: compared with direct integration, a speed up factor of more than ten combined with an relative error in temperature of about 1% was found.

NOMENCLATURE

symbol	description	unit
A	activator	
$\mathbf{A}$	reaction mapping Jacobian	[1/s]
C_p	specific heat	[kJ/(kg K)]
E_a	activation energy	[kJ/kmol]
I	initiator	
$\mathbf{J}$	chemical source term Jacobian	[1/s]
M	monomer	
N_I	number of initiators	
N_p	number of particles	
N_s	number of species	
N_t	number of time steps	
P	polymer	
R	radical	
$\mathbf{R}$	reaction mapping operator	[kmol/m^3]
R_g	gas constant	[kJ/(kmol K)]
$\mathbf{S}$	source vector	[kmol/(m^3 s)]
T	temperature	[K]
V_a	activation volume	[kJ/(kmol atm)]
f	fraction of monomer at inlet	
f_{mix}	mixing frequency $1/\tau_{\text{mix}}$	
k	reaction rate	[1/s or m^3/(kmol s)]
k_0	preexponential factor	[1/s or m^3/(kmol s)]
p	pressure	[atm]

*Address all correspondence to this author: eelco@iastate.edu

t	time	[s]
ΔH	enthalpy change	[kJ/kmol]
Δt	numerical time step	[s]
ε_L	mapping error	[kmol/m^3]
ϕ	composition vector of species	[kmol/m^3]
λ_i	i^{th} moment of R	
μ_i	i^{th} moment of P	
ρ	density of monomer	[kg/m^3]
τ_{mix}	mixing time scale	[s]
τ_{pair}	pairing time scale	[s]
τ_{res}	residence time	[s]

INTRODUCTION

Turbulent mixing of fast, exothermic reactants dissolved in initially segregated liquids represent a broad range of processes in industry. A typical example taken representative in this research is the production of low-density polyethylene (LDPE). Due to the commercial competence and the large production volumes involved, LDPE has traditionally been an important research topic in industry. LDPE is commonly manufactured in a tubular reactor which is filled with monomer. One or multiple feed pipes are used to add a small stream of initiator to start the polymerization process. The process condition of the feed stream downstream from the injector may strongly influence the polymerization process, as there is a strong coupling between the chemical kinetics and hydrodynamics: the kinetics are highly exothermic, and the reaction rate constants have a strong non-linear dependence to the temperature. Poor micro-mixing conditions in the reactor may lead to formation of hot-spots, and, as a result, to degrading of the polymer quality due to the formation of high mass-density polymer chains (Kolhapure and Fox, 1999).

Computational fluid dynamics (CFD) is an important tool for prediction of hot-spot formation in LDPE reactors for given process conditions. Since the flow in many industrial reactors is non-homogeneous and time-dependent, a three-dimensional (3-D), transient solution of the turbulent reacting flow is desirable. For the fluid motion, this is (with the current computational resources) well feasible by using a large eddy simulation (LES) approach: the transport equation of the low-pass filtered fluid is solved explicitly, and the influence of the non-resolved subgrid scales (SGS) to the large scales is modeled. The closure models are assumed to be geometry independent, since they apply on the smallest turbulent scales only. As a result, LES has successfully been applied to turbulent flows in a broad range of process equipment, such as stirred tanks reactors, gas cyclones and crystallizers. Implementation of chemistry into LES, however, is difficult due to the usually highly non-linear behavior of the chemical source term, which is hard to capture adequately by a subgrid scale model.

A relatively new approach for treatment of chemistry in LES is the filtered density function (FDF) technique (Pope, 1990). The FDF methodology solves the transport equation of the probability density function (PDF) of the low-pass filtered scalars. In this way, the reacting scalars can be incorporated into a large eddy simulation of the flow in the reactor without the need to model the filtered reaction rate term, since this remains closed. Colucci et al. (1998) applied the FDF methodology to a temporally developing mixing layer and a spatially developing planar jet under both non-reacting and reacting (single reaction) conditions, and showed close agreement with DNS results. Variable density was included by Jaberi et al. (1999). Van Vliet et al. (2001) extended the FDF method to parallel, competitive reactions of the type $\mathcal{A} + \mathcal{B} \rightarrow \mathcal{P}$ and $\mathcal{A} + \mathcal{C} \rightarrow \mathcal{Q}$ (with the reaction rates in the ratio $k_1 : k_2 = 1000 : 1$), and demonstrated that the dependency of the yield on the Damköhler number (Da) was qualitatively well predicted.

In spite of the promising results of FDF/LES, the major draw back remains the computational costs involved to obtain a solution of the FDF/LES transport equation. Usually, a Lagrangian Monte Carlo (MC) solver is used (Pope, 1985): many fictitious MC particles representing the full local composition vector $\phi \equiv \phi_i (i = 1 \ldots N_s + 1)$ of the species are tracked in the LES flow field, obeying stochastic differential equations which are chosen such that the FDF equation is recovered in a statistical sense. In order to obtain sufficient statistical accuracy, typically fifty particles per computational grid cell are tracked, and as a result, in case of full 3-D simulation more than ten million particles are required. Van Vliet et al. (2003) performed FDF/LES in a turbulent reactor in the vicinity of the injector. In their simulations, more than 60 million particles were tracked on a $80 \times 80 \times 400$ computational grid. In this way, a parallel cluster of 22 CPU's was kept busy for almost three months. Three-dimensional FDF/LES is therefore feasible only if the computational time of the chemistry is relatively short. In case of fast complex chemistry such as LDPE, however, much more CPU time is required to solve the chemistry at each MC particle by direct integration. For LDPE, the CPU time to calculate the chemistry is about 0.12 ms per particle on a 800MHz Alpha processor. For the tubular reactor, this implies that a total CPU time of about $60 \times 10^6 \times 0.12 \times 10^{-3} = 7680$ s per computational time step is needed. On a parallel cluster of 20 CPU's, it would take more than a month in order to calculate a single macro time scale (8000 time steps). Obviously, FDF/LES is currently not feasible in a three-dimensional LDPE reactor without the use of more efficient ways to treat the chemistry at each notional particle.

Pope (1997) developed a new computational technique for calculating complex chemistry that reduces the required CPU time significantly compared to even the most efficient ordinary differential equation (ODE) solver. The method is based on *in situ* adaptive tabulation (ISAT) of the accessed region of the composition space. Every outcome of chemical reactions obtained by direct integration using an ODE solver is stored in a table. Since the table is built 'on the fly' during a calculation,

only regions of the composition space that are actually used are stored, resulting in relatively small table for even a large number of species[1]. ISAT has successfully been applied to numerous applications which require a large number of evaluations of a stiff set of ODE's (e.g. Raman and Fox, 2001; Kolhapure and Fox, 1999; Wang and Fox, 2003). In the present research, we use the latest version 4.0 of ISAT (Pope, 2003) for the full LDPE reaction scheme that was proposed by Zhou et al. (2001). The aim was to optimize ISAT in terms of speed up and accuracy with respect to direct integration using a conventional ODE solver by varying the error tolerance and number of trees. Ultimately, LDPE has to be implemented into a full 3-D FDF simulation, so significant speed up is required. In this paper, however, we will use a pairwise mixing stirred reactor (PMSR) algorithm (Pope, 1997) in order to mimic the effect of turbulent mixing on the MC particle, since virtually all computational time now can be attributed to the chemistry evaluations. Furthermore, mixing in the PMSR is known to be a more stringent test for chemistry solvers due to its discontinuous way of accessing composition space.

The layout of the remainder of the paper is as follows. Firstly, some theoretical background of the ISAT algorithm is given. Next, the LDPE kinetics are introduced that need to be solved by ISAT. Then, the PMSR algorithm is described. In the results section, the performance of the ISAT algorithm in terms of speedup and accuracy is presented. Finally, the conclusions are given.

IN SITU ADAPTIVE TABULATION (ISAT)

ISAT (Pope, 1997) is a relatively novel chemistry tabulation algorithm for handling complex reactions. In this section, a short outline of ISAT is given in order to be able understand the terminology in the rest of the paper.

The composition of N_s reacting scalars evolve according to

$$\frac{d\phi}{dt} = \mathbf{M}(\phi(t)) + \mathbf{S}(\phi(t)), \tag{1}$$

where the first term is the rate of change of the composition vector ϕ due to transport, and the second term is the rate of change due to chemical reactions. The transport term is treated by the PMSR (see next the section), whereas ISAT takes care of the reaction term. The solution due the chemical reactions (i.e. if $\mathbf{M} = 0$ is assumed) after a fixed time step Δt of equation (1) for a certain initial state ϕ_0 is called the reaction mapping $\mathbf{R}$. In figure 1, the exact mapping of $\phi_0^{[i]} \longrightarrow \phi_{\Delta t}^{[i]}$ (lowest curve in figure 1) is

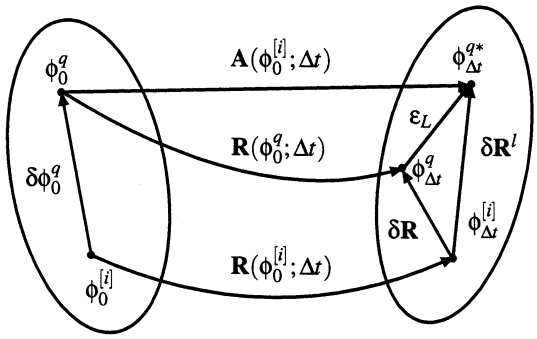

Figure 1. Linearized mapping in ISAT (obtained from Fox, 2003)

indicated by $\mathbf{R}(\phi_0^{[i]};\Delta t)$. It is assumed that this exact mapping is stored at a node i, denoted as a *leaf*.

Suppose that another mapping is needed (called a *query*) for a composition $\phi^{(q)}$ with a small displacement $\delta\phi$ from $\phi^{[i]}$:

$$\phi_0^q = \phi_0^{[i]} + \delta\phi. \tag{2}$$

The exact reaction mapping corresponding to $\phi^{(q)}$ is

$$\mathbf{R}(\phi_0^q;\Delta t) = \mathbf{R}(\phi_0^{[i]};\Delta t) + \delta\mathbf{R} \tag{3}$$

(middle curve in figure 1). This reaction mapping can be approximated by linear interpolation as

$$\mathbf{R}(\phi_0^q) \approx \mathbf{R}^l(\phi_0^q) \equiv \mathbf{R}(\phi_0) + \delta\mathbf{R}^l \tag{4}$$

(upper line in figure 1), where

$$\delta\mathbf{R}^l \equiv \mathbf{A}\delta\phi = \delta\mathbf{R} + O(|\delta\phi^2|), \tag{5}$$

and the mapping gradient matrix $\mathbf{A}(\phi_0)$ (stored at leaf i) is

$$A_{ij}(\phi) \equiv \frac{\partial R_i(\phi)}{\partial \phi_j}. \tag{6}$$

It can be shown (Pope, 1997), that the mapping reaction gradient $\mathbf{A}$ is related to the chemical source term Jacobian $\mathbf{J} \equiv J_{ij} = dS_i/d\phi_j$ via the matrix exponential[2]

$$\mathbf{A}(\phi_0) = \mathrm{expm}(\mathbf{J}\Delta t), \tag{7}$$

so that $\mathbf{A}$ can be obtained from chemical source term vector $\mathbf{S}$.

[1] In contrast to conventional chemical lookup tables, which are created in a preprocessing step and thus need to cover the whole chemical composition space. Since the composition space grows exponentially with the number of chemical components, the conventional chemical lookup table technique is only feasible for a small amount of species.

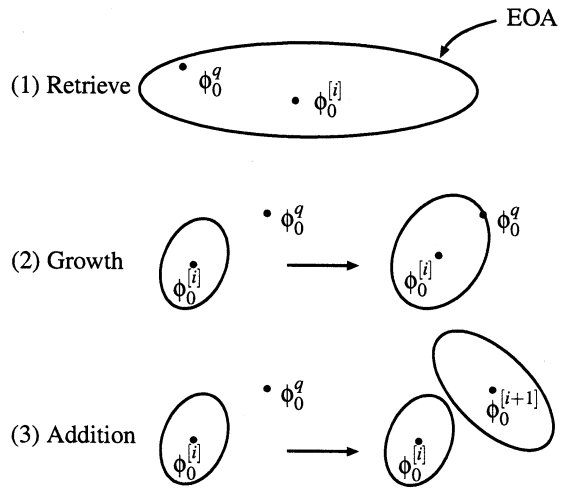

Figure 2. Schematic representation the three events in ISAT after a query: (1) Retrieve, (2) Growth, and (3) Addition (from Fox, 2003).

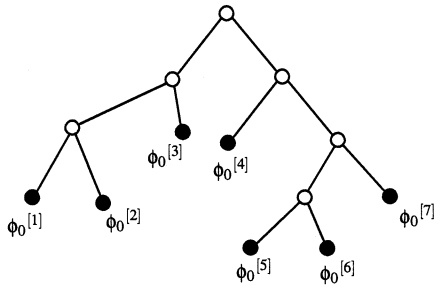

Figure 3. Sketch of the binary tree as build by ISAT. Each filled dot is a record; at each open dot a cutting plane is defined (from Pope, 1997).

Pope (1997) shows that the error $\varepsilon_L \equiv \phi^{q*}_{\Delta t} - \phi^{q}_{\Delta t}$ is bounded by the ellipsoid of accuracy (EOA) according to

$$0 \le \delta\phi_0{}^T \mathbf{V}_A \tilde{\Sigma}_A{}^T \tilde{\Sigma}_A \mathbf{V}_A^T \delta\phi_0 \le \varepsilon_{\text{tol}}^2, \tag{8}$$

where $\mathbf{V}_A$ and $\tilde{\Sigma}_A$ are the unitary matrix and singular value diagonal matrix of the singular value decomposition $A = \mathbf{U}_A \tilde{\Sigma}_A \mathbf{V}_A^T$. For a predefined error tolerance ε_{tol}, the query ϕ_0^q is inside the EOA if equation (8) is satisfied.

The ISAT algorithm now is a follows. A certain query ϕ_0 is compared with respect to the closest leaf $\phi^{[i]}$ that was previously calculated by DI. The three events that may occur are shown in figure 2:

[2]The matrix exponential of matrix **A** is defined in terms of power series expansion as $\text{expm}(\mathbf{A}) = \mathbf{I} + \mathbf{A}^2/2 + \mathbf{A}^3/3! \ldots$.

Table 1. Reaction rate constants of LDPE kinetics given by eq. (9)

	k_0 [a]	E_a [kJ/kmol]	V_a [kJ/(kmol atm)]
k_{di}	6.639×10^{15}	1.56×10^5	0.2533
k_{i}	5.887×10^7	2.97×10^4	−2.403
k_{p}	5.887×10^7	2.97×10^4	−2.403
k_{trm}	5.823×10^5	4.62×10^4	−2.092
k_{td}	1.075×10^9	1.25×10^3	−1.468
k_{tc}	1.075×10^9	1.25×10^3	−1.468

[a] 1/s and m^3/(kmol s) for first and second order reactions, resp.

1. **Retrieve**: The query is inside the EOA, and the reaction mapping is *retrieved* by using linear interpolation (eq. 4).
2. **Growth** The query is outside the current EOA, and the mapping is obtained by DI. The exact error ε_L which now is available, appears to be below the predefined error tolerance, and the EOA is *grown* to include the query.
3. **Addition** The query is outside the current EOA, and the exact reaction mapping is found by DI. The exact error ε_L appears to be larger than the predefined error tolerance, and a new leaf $i+1$ is *added* at $\phi^{(q)}$.

Following this algorithm, a binary tree containing the leafs $\phi^{[i]}$ is built (see figure 3). For each query, the tree is searched for the leaf with its value closest to the query. This node is used to obtained the reaction mapping via retrieve, growth, or addition. ISAT initially needs to do DI's in order to create a tree by growing and adding leafs. As the tree becomes bigger, however, more and more queries are retrieved by linear interpolation, and the mapping of chemical reaction becomes more and more efficient. More speed up and accuracy can be obtained by building multiple trees, although an optimum probably exists. The optimal number of trees, N_{tree}, for our particular reaction is also investigated in this paper.

LDPE KINETICS

In the present research, we study high pressure free-radical polymerization. We base our kinetics on a simplified LDPE reaction scheme that resembles the one given by Tsai and Fox (1996)

Table 2. Physical constants

specific mass	ρ	444	$[\mathrm{kg/m^3}]$
specific heat	C_p	2.51	[kJ/(kg K)]
enthalpy	ΔH	95.0	[kJ/kmol]
Gas constant	R_g	8.31	[kJ/(kmol K)]

and Zhou et al. (2001):

$$
\begin{aligned}
&\text{Initiator decomposition} && I_i \xrightarrow{k_{di}} 2A \qquad (i = 1 \ldots N_I)\\
&\text{Chain initiation} && A + M \xrightarrow{k_i} R_1\\
&\text{Propagation} && R_n + M \xrightarrow{k_p} R_{n+1}\\
&\text{Chain transfer to monomer} && R_n + M \xrightarrow{k_{trm}} P_n + R_1\\
&\text{Disproportionation termination} && R_n + R_m \xrightarrow{k_{td}} P_n + P_m\\
&\text{Combination termination} && R_n + R_m \xrightarrow{k_{tc}} P_{n+m}.
\end{aligned}
\tag{9}
$$

No quasi steady state assumption has been applied. The reaction rates k are given by the Arrhenius relation

$$
k = k_0 \exp\Big(-\frac{E_a + V_a p}{R_g T}\Big), \tag{10}
$$

where k_0 is the preexponential factor, E_a is the activation energy, V_a is the activation volume, p is the pressure, R_g is the universal gas constant and T is the temperature. The same Arrhenius constants (see table 1) as Tsai and Fox (1996) and Zhou et al. (2001) were used. This kinetic scheme includes initiation, propagation, termination by disproportionation, termination by combination, and finally, chain transfer to monomer. Other mechanisms, such as backbiting, scission of radicals and retardation of impurities are not considered as these are not important for predicting the monomer conversion and polydispersity (Zhou et al., 2001). The general case of N_I initiators I_i is assumed, each with its own activation energy. In this paper, $N_I = 1$, but in future work the number of initiators will be varied. The initiators decompose into two free radicals (A) per initiator molecule. Free radicals react with monomer M to a radical of unit length R_1, which propagate by the addition of M to form a free radical of length R_n. Termination occurs when two radical of length n and m react to form a dead polymer of length $n+m$ (termination by combination), or to form two dead polymers of length n and m (termination by disproportionation).

Table 3. Operating conditions PMSR

Inlet temperature	T	500	[K]
Inlet monomer mass fraction	f	.999	[-]
Inlet monomer concentration	$[M]$	15.87	$[\mathrm{kmol/m^3}]$
Inlet initiator concentration	$[I]$	1.4	$[\mathrm{kmol/m^3}]$
Pressure	p	2,500	[atm]

The moments of the radicals and polymers are defined as

$$
\begin{aligned}
&\lambda_0 = \textstyle\sum_{n=1}^{\infty} R_n \qquad \lambda_1 = \sum_{n=1}^{\infty} n R_n \qquad \lambda_2 = \sum_{n=1}^{\infty} n^2 R_n\\
&\mu_0 = \textstyle\sum_{n=1}^{\infty} P_n \qquad \mu_1 = \sum_{n=1}^{\infty} n P_n \qquad \mu_2 = \sum_{n=1}^{\infty} n^2 P_n,
\end{aligned}
\tag{11}
$$

where n is the number of radicals or polymer in a chain, and λ_i and μ_i is the i^{th} moment of the radicals and polymers, respectively. By using the methods of moments (Kiparissides et al., 1997), the reaction rate vector can be written in terms of the moments of the radicals and polymers according to

$$
\begin{aligned}
S_{Ii} &= -k_{di}[I_i] \quad (i = 1 \ldots N_I)\\
S_A &= 2\sum_{i=1}^{N_I} k_{di}[I_i] - 2k_i[A][M]\\
S_M &= -k_i[A][M] - k_p\lambda_0[M] - k_{trm}\lambda_0[M]\\
S_{\lambda_0} &= S_R = -(k_{td} + k_{tc})\lambda_0^2 + k_i[A][M]\\
S_{\mu_0} &= S_P = -(k_{td} + \tfrac{1}{2}k_{tc})\lambda_0^2 + k_{trm}[\lambda_0][M]\\
S_{\lambda_1} &= -(k_{td} + k_{tc})\lambda_0\lambda_1 + k_i[A][M] + k_p\lambda_0[M]\\
&\quad + k_{trm}[M](\lambda_0 - \lambda_1)\\
S_{\lambda_2} &= -(k_{td} + k_{tc})\lambda_0\lambda_2 + k_i[A][M] - k_p\lambda_0[M]\\
&\quad + k_{trm}[M](\lambda_0 - \lambda_2) + 2k_p\lambda_1[M]\\
S_{\mu_1} &= (k_{td} + k_{tc})\lambda_0\lambda_1 + k_{trm}\lambda_1[M]\\
S_{\mu_2} &= (k_{td} + k_{tc})\lambda_0\lambda_2 + k_{trm}\lambda_2[M] + k_{tc}\lambda_1^2\\
S_T &= \Big(\frac{\Delta H}{\rho C_p}\Big)k_p\lambda_0[M],
\end{aligned}
\tag{12}
$$

where the bracket quantities are the species concentration in $\mathrm{kmol/m^3}$. The last source term is the enthalpy balance that assumes that the heat release can be completely attributed to the propagation step (Kiparissides et al., 1997). Here, ρ is the density of the reaction mixture, ΔH is the enthalpy change for monomer propagation, and C_p is the heat capacity of monomer. The physical constants and inlet condition used in this research are summarized in table 2 and 3.

Table 4. Numerical settings of the PMSR for cases with varying mixing time.

Case	1	2	3	4	5	6
τ_{mix}	0.1	0.05	0.01	$5\cdot10^{-3}$	$2\cdot10^{-3}$	10^{-3}
τ_{pair}	1	0.5	0.1	0.05	0.02	0.01
Δt	0.01	$5\cdot10^{-3}$	10^{-3}	$5\cdot10^{-4}$	$2\cdot10^{-4}$	10^{-4}
N_t	100	200	10^3	$2\cdot10^3$	$5\cdot10^4$	10^4
N_p	$4\cdot10^4$	$2\cdot10^4$	$4\cdot10^3$	$2\cdot10^3$	800	400

Finally, the polydispersity is defined as

$$Z_p = \frac{\mu_0\mu_2}{\mu_1^2}. \tag{13}$$

PAIRWISE MIXING STIRRED REACTOR

The pairwise mixing stirred reactor (PMSR) is used in this research to optimize the CPU time of the solver for the LDPE reactions. It was developed by Pope (1997) in order to mimic turbulent reactive mixing (i.e. the first term in equation 1). The PMSR is able to create a large accessed region in composition space, and therefore, it forms a stringent test for the performance of the chemistry solver.

The PMSR consists of an even number of particles N_p. The i^{th} particle has a composition at time t of $\phi^{[i]}(t)$. At every discrete time step $k\Delta t$, a discontinuous change of ϕ is established due to *inflow*, *outflow*, and *pairing*. In between these discrete steps, the composition changes continuously due to *mixing* and *reaction*. The particles are arranged in pairs, such that particle 1 and 2, 3 and 4,... $N_p - 1$ and N_p, are partner. During the mixing fractional time step, each pair of particles, say p and q, evolve according to

$$\begin{aligned} \frac{d\phi^{(p)}}{dt} &= -(\phi^{(p)} - \phi^{(q)})/\tau_{mix} \\ \frac{d\phi^{(q)}}{dt} &= -(\phi^{(q)} - \phi^{(p)})/\tau_{mix} \end{aligned} \tag{14}$$

Every time step, inflow and outflow is established by setting $\frac{1}{2}N_p\Delta t/\tau_{res}$ pairs to the inlet composition and temperature, so that on average the residence time of each particle is τ_{res}. At the same time, $\frac{1}{2}N_p\Delta t/\tau_{pair}$ pairs are selected (different from the in and outflow) which are randomly shuffled, such that all particles are likely to change partners. In this way, a discontinuous change of composition with a time scale τ_{pair} is established.

RESULTS

The performance of ISAT in terms of accuracy and speed up is studied for mixing times varying from $\tau_{mix} = 0.1\tau_{res}$ (poorly mixed) to $\tau_{mix} = 0.001\tau_{res}$ (well mixed). The residence time was kept constant to $\tau_{res} = 1$. The pairing time τ_{pair} and the numerical time step were kept in a fixed ratio $\tau_{pair}/\tau_{mix} = \tau_{mix}/\Delta t = 10$, so that number of time step per residence time scale varies with the mixing time as $N_t = 10\tau_{res}/\tau_{mix}$. The total number of ODE evaluations per residence time scale was kept constant by setting $N_pN_t = 4\times10^6$. The numerical settings are summarized in table 4. A Livermore solver for ordinary differential equations with automatic method switching for stiff and non-stiff problems (Hindmarsh, 1983) was used for the exact solution of the LDPE kinetics. The error tolerance was taken to be 10^{-6} (smaller tolerance virtually gave the same result). The matrix exponential needed for the mapping matrix (eq. 7) was obtained with the reducible rational Pade approximation (Sidje, 1998). Before the ISAT results are presented, first the behavior of LDPE in the PMSR is studied by using the exact ODE solver.

An impression of the temperature and polydispersity variation in time at a single pair of particles in the reactor is given in figure 4. The PDF obtained from all particles in the reactor is shown at the right side of each figure. A poorly mixed system with $\tau_{mix} = 0.1\tau_{res}$ (fig. 4a and 4b) is compared with a well mixed system with $\tau_{mix} = 0.001\tau_{res}$. (fig. 4c and 4d). In both cases, the majority of the particles have a temperature equal to the operating temperature of about 680 K, reflected by the primary narrow peak in the PDF at this temperature. On an average of one time per residence time, the temperature is initialized to the inlet temperature of 500 K. In the poorly mixed system, it takes about $0.5\tau_{res}$ to get back to operating temperature after being initialized. Moreover, the temperature shows a small temperature fluctuation above the mean operating temperature at every final stage of reaction. In the temperature PDF, these fluctuations are reflected by the broadening of the peak at the operating temperature to higher values. In the polydispersity PDF this broadening is even more pronounced, as Z_p is highly sensitive to the local temperature. Since the fluctuations are not present in the well mixed system, these are attributed to hot-spot formation due to poor micro mixing condition, which also was observed by Kolhapure and Fox (1999) and Zhou et al. (2001). Note furthermore the secondary peak in the temperature PDF of the well mixed system (figure 4c), which is located half way the inlet and operating temperature. This peak is an artifact due to the discontinuous pairing in the PMSR: a initialized particle that is introduced into the system is likely to pair on a short time scale (because τ_{pair} is small) with a particle having the operating temperature (because these are in majority). The short mixing time causes a quick approach to their average temperature half way the inlet and operating temperature.

The accuracy and speed up of ISAT is studied in figure 5 by comparing the relative error in temperature and polydisper-

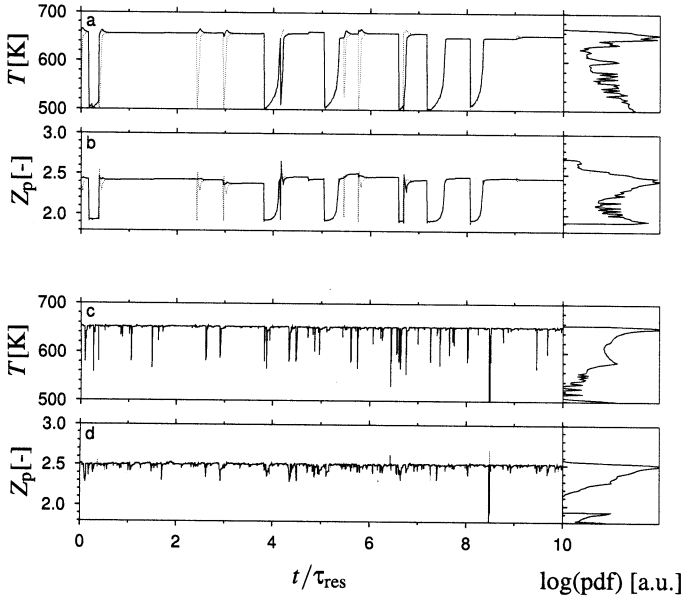

Figure 4. Temperature and polydispersity vs time, monitored at a pair of particles p and q (solid and dotted line) for $\tau_{\text{mix}} = 0.1\tau_{\text{res}}$ (a and b) and $\tau_{\text{mix}} = 0.001\tau_{\text{res}}$ (c and d). The probability density function at the right side is obtained from all particles in the reactor averaged over twenty residence time scales.

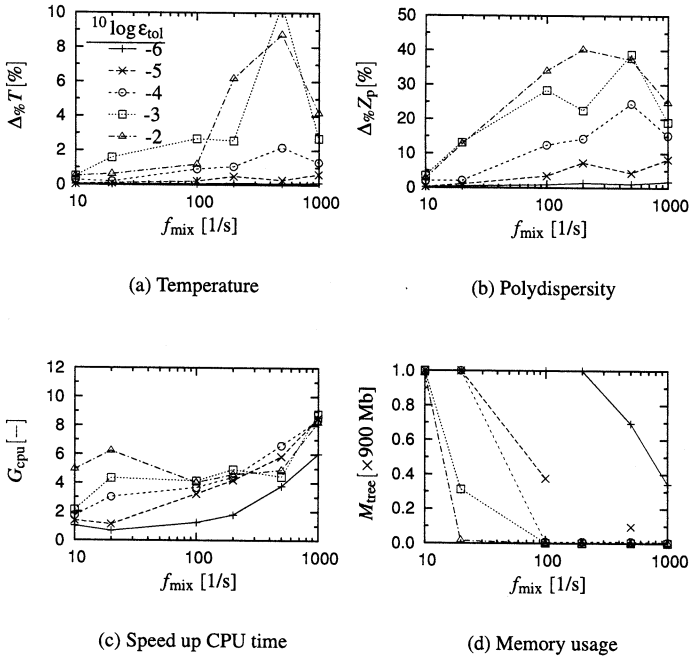

(a) Temperature (b) Polydispersity

(c) Speed up CPU time (d) Memory usage

Figure 5. Sensitivity to the mixing frequency $f_{\text{mix}} = 1/\tau_{\text{mix}}$ of (a) the relative error in temperature: $\Delta_{\%}T = 100(T_{\text{isat}} - T_{\text{ode}})/T_{\text{ode}}$, (b) the relative error in polydispersity: $\Delta_{\%}Z_{\text{p}} = 100(Z_{\text{p}_{\text{isat}}} - Z_{\text{p}_{\text{ode}}})/Z_{\text{p}_{\text{ode}}}$, (c) the ISAT speed up factor: $G_{\text{cpu}} = \mathcal{T}_{\text{ode}}/\mathcal{T}_{\text{isat}}$, and (d) the ISAT memory usage: M_{tree}, for five different ISAT error tolerances $^{10}\log\varepsilon_{\text{tol}}$: -6 (pluses), -5 (crosses), -4 (circles), -3 (squares), and -2 (triangles). The number of trees was taken to be $N_{\text{tree}} = 2$.

sity (with respect to the solution obtained by DI, see figure 5) for varying mixing frequency $f_{\text{mix}} = 1/\tau_{\text{mix}}$, and for five different error tolerances ε_{tol} (equation 8). The number of trees was taken $N_{\text{tree}} = 2$. Figure 5(a) shows that the temperature is reasonably well ($\Delta_{\%}T < 2$) predicted for mixing frequencies smaller than 100 for all error tolerances. The smallest error tolerance $\varepsilon_{\text{tol}} = 10^{-6}$ yields an exact result. For $f_{\text{mix}} > 100$, only $\varepsilon_{\text{tol}} \leq 10^{-5}$ give acceptable accuracy. The polydispersity (shown in figure 5(b)) is in general less accurately predicated (note the difference in scales). For error tolerances smaller than 10^{-5}, the accuracy is smaller than 10%. The speed up G_{cpu} (defined as the ratio of the CPU time per time step needed by ODE solver and ISAT) is shown in figure 5(c). No speed up is obtained by ISAT for mixing frequency smaller than 100. Figure 5(d) shows that in this case, the maximum memory of 900 Mb is used. Apparently, for this error tolerance, the EOA is so small that hardly any retrieves are obtained. For $f_{\text{mix}} > 100$, the speed up increases up to a factor six for $f_{\text{mix}} = 1{,}000$. For $\varepsilon_{\text{tol}} = 10^{-5}$, the largest speed

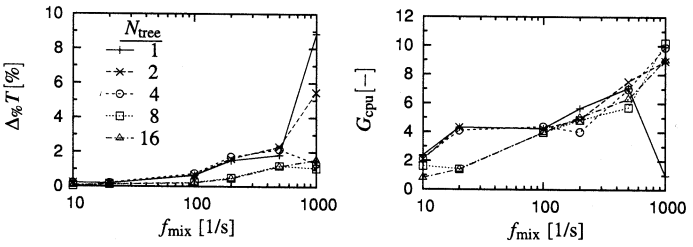

(a) Temperature (b) Speed up CPU time

Figure 6. Sensitivity to the mixing frequency $f_{\text{mix}} = 1/\tau_{\text{mix}}$ of (a) the relative error in temperature and (b) the ISAT speed up factor for five different number of trees N_{tree}: 1 (pluses), 2 (crosses), 4 (circles), 8 (squares), and 16 (triangles). The error tolerance was $\varepsilon_{\text{tol}} = 10^{-4}$ for $f_{\text{mix}} \leq 100$ and $\varepsilon_{\text{tol}} = 10^{-5}$ for $f_{\text{mix}} > 100$. See figure 5 for the error definitions.

up is a factor eight. In conclusion, the speed up and accuracy depend on the mixing frequencies: higher mixing frequencies give better results. The error tolerance $\varepsilon_{tol} = 10^{-6}$ is too small to give significant speed up. For $f_{mix} > 100$, the error tolerance $\varepsilon_{tol} = 10^{-5}$ shows acceptable accuracy ($\Delta_{\%}T < 1$, $\Delta_{\%}Z_p < 10$) combined with significant speed up ($G_{cpu} = 8$). For $f_{mix} \leq 100$, $\varepsilon_{tol} = 10^{-5}$ is still accurate, but without speed up. In this region, $\varepsilon_{tol} = 10^{-4}$ should be taken: an accuracy smaller than 2% combined with a speed up factor $G_{cpu} = 4$ is obtained.

In figure 6, the number of trees, N_{tree}, is varied for the fixed error tolerance recommended above ($\varepsilon_{tol} = 10^{-4}$ for $f_{mix} \leq 100$ and $\varepsilon_{tol} = 10^{-5}$ for $f_{mix} > 100$). In figure 6(a), it is shown that the best overall accuracy is obtained by taking four or more trees, especially for $f_{mix} > 100$. Figure 6(b) shows that also the speedup is largest for $N_{tree} \geq 4$. The best results are obtained by taking $N_{tree} = 8$, yielding an accuracy of 1% in temperature combined with an speed up factor of more than ten for $f_{mix} = 1,000$.

CONCLUSIONS

A low density polyethylene (LDPE) reaction scheme was implemented in a pairwise mixing stirred reactor (PMSR). In situ adaptive tabulation (ISAT V4.0, Pope, 2003) was used for the evaluation of the ordinary differential equations (ODE's) describing the LDPE kinetics. The aim was to optimize ISAT in terms of speed-up and accuracy with respect to direct integration. For this purpose, the error tolerance ε_{tol} and the number of trees N_{tree} used in ISAT were varied, and the speed-up and relative error of the species were determined for a range of mixing frequencies of the PMSR. Overall, the highest speed-up combined with the best accuracy was obtained by taking $N_{tree} = 8$ and $\varepsilon_{tol} = 10^{-5}$, yielding a speed-up factor of more than ten combined with a relative error of about 1% for a mixing frequency $f_{mix} = 1,000$. These settings are taken as a guide line for the implementation of LDPE in an 3-D FDF/LES simulation of a tubular reactor. It is expected, however, that in real turbulent flows the restrictions on the error tolerance are somewhat relaxed, and, furthermore, that more speed-up is gained, since mixing in PMSR is known to be a stringent test for chemistry solvers due to its discontinuous way of accessing composition space. In the FDF/LES simulation, it is therefore worthwhile to check if more speed up (with adequate accuracy) can be obtained by choosing a larger error tolerance.

ACKNOWLEDGEMENT

We gratefully acknowledge the support of SABIC EuroPetrochemicals.

REFERENCES

Colucci, P. J., Jaberi, F. A., Givi, P., and Pope, S. (1998). Filtered density function for large eddy simulation of turbulent reacting flows. *Phys Fluids*, 10(2):499–515.

Fox, R. O. (2003). *Computational models for turbulent reacting flows*. Cambridge University Press.

Hindmarsh, A. C. (1983). ODEPACK, *A Systematized Collection of ODE Solvers*, pages 55–64. R. S. Stepleman et al. (Eds.).

Jaberi, F. A., Colucci, P. J., James, S., Givi, P., and Pope, S. B. (1999). Filtered mass density function for large-eddy simulation of turbulent reacting flows. *J. Fluid Mech.*, 401:85–121.

Kiparissides, C., Achilias, D. S., and Sidiropoulou, E. (1997). Dynamic simulation of industrial poly(vinyl chloride) batch suspension polymerization reactors. *Ind. Eng. Chem. Res.*, 36(4):1253.

Kolhapure, N. H. and Fox, R. O. (1999). CFD analysis of micromixing effects on polymerization in tubular low-density polyethylene reactors. *Chem. Eng. Sci.*, 54:3233–3242.

Pope, S. B. (1985). Pdf methods for turbulent reactive flows. *Prog. Energy Combust. Sci.*, 11:119–192.

Pope, S. B. (1990). Computations of turbulent combustion: Progress and challenges. *Proc. Combust. Inst.*, 23:591–612.

Pope, S. B. (1997). Computational efficient implementation of combustion chemistry using in situ adaptive tabulation. *Combust. Theory Modeling*, 1:41–63.

Pope, S. B. (2003). ISATAB V4.0. *In Situ Adaptive TABulation. User Manual.*

Raman, V. and Fox, R. O. (2001). CFD analysis of premixed methane chlorination reactors with detailed chemistry. *Ind. Eng. Chem. Res.*, 40:5170–5176.

Sidje, R. B. (1998). EXPOKIT. Software Package for Computing Matrix Exponentials. *ACM Trans. Math. Softw.*, 24(1):130–156.

Tsai, K. and Fox, R. O. (1996). Pdf modeling of turbulent-mixing effects on initiator efficiency in a tubular reactor. *AIChe Journal*, 42:2926–2940.

Van Vliet, E., Derksen, J. J., and Van den Akker, H. E. A. (2001). Modelling of parallel competitive reactions in isotropic homogeneous turbulence using a filtered density function approach for large eddy simulations. In *Proc. of the 3rd Int. Symp. on Comp. Techn. for Fluid/Thermal/Chemical Systems with Industrial Appl.*, Atlanta, Georgia, USA.

Van Vliet, E., Derksen, J. J., and Van den Akker, H. E. A. (2003). Turbulent reactive mixing in a tubular reactor: An FDF/LES approach. *AIChE Journal*. Submitted.

Wang, L. and Fox, R. O. (2003). Application of in situ adaptive tabulation to CFD simulation of nano-particle formation by reactive precipitation. *Chem. Eng. Sci.*, 58:4378–4401.

Zhou, W., Marshall, E., and Oshinowo, L. (2001). Modeling LDPE tubular and autoclave reactors. *Ind. Eng. Chem. Res.*, 40:5533–5542.